INSTITUTE FOR FUSION STUDIES

DOE/ET-53088-505 IFSR #505

Shock Formation in a Poloidally Rotating Tokamak Plasma

K.C. SHAING
Oak Ridge National Lab.
Oak Ridge, Tennessee 37831-8071
R.D. HAZELTINE
Institute for Fusion Studies
The University of Texas at Austin
Austin, Texas 78712
and
H. SANUKI
National Institute for Fusion Science
University of Nagoya
Nagoya, Japan

June 1991

THE UNIVERSITY OF TEXAS

AUSTIN

Shock formation in a poloidally rotating tokamak plasma*

K. C. Shaing
Oak Ridge National Laboratory, Oak Ridge, Tennessee 37831-8071

R. D. Hazeltine
Institute for Fusion Studies, The University of Texas at Austin,
Austin, Texas 78712

H. Sanuki
National Institute for Fusion Science, University of Nagoya,
Nagoya, Japan

ABSTRACT

When the Mach number M_p of the poloidal rotation in a tokamak approaches unity, the poloidal variations of plasma density and potential appear to have the characteristics of a shock whose front lies on a plane (ribbon) of a fixed poloidal angle η_0. The shock first appears, when $1 - M_p \lesssim \sqrt{\epsilon}$ (ϵ is the inverse aspect ratio), on the inside of the torus at a shock angle $\eta_0 \geq \pi$ if the plasma rotates counterclockwise poloidally. As M_p increases, η_0 moves in the direction of the poloidal rotation. At $M_p = 1$, $\eta_0 = 2\pi$. When $M_p - 1 \lesssim \sqrt{\epsilon}$, the shock angle is at $\eta_0 \lesssim \pi$. The parallel viscosity associated with the shock is collisionality independent, in contrast to the conventional neoclassical viscosity. The viscosity reaches its maximum at $M_p = 1$, which is the barrier that must be overcome to have a poloidal supersonic flow. Strong up-down asymmetric components of poloidal variations of plasma density and potential develop at $M_p \simeq 1$. In the edge region, the convective poloidal momentum transport weakens the parallel viscosity and facilitates the transition from L-mode to H-mode.

PACS numbers: 52.25.Fi; 52.55.Fa.

* Research sponsored by the Office of Fusion Energy, U.S. Department of Energy, under contract DE-AC05-84OR21400 with Martin Marietta Energy Systems, Inc., and under contract DE-FG05-80ET-53088 with the University of Texas at Austin.

I. INTRODUCTION

Since the observation of the transition from L-mode to H-mode,[1] many theories have been proposed to explain the phenomenon.[2-6] Theories based on the radial electric field E_r seem especially in accord with the available experimental data.[4-6] The main thrust of these theories is that the anomalous transport fluxes are influenced by E_r and dE_r/dr. Here r is the minor radius. Sudden changes in these variables trigger the L-H transition, which subsequently suppresses turbulent fluctuations and improves plasma confinement. Experimental measurements in CCT and DIII-D, motivated by the theories, show that indeed E_r and dE_r/dr change suddenly at the onset of the transition and are related to the change of the poloidal flow velocity V_p.[7,8] A bifurcation theory of poloidal rotation has been developed based on the nonlinearity of the parallel (or poloidal) viscosity.[9] The main reason for the bifurcation is the existence of a local maximum in the parallel viscosity. However, both theoretically predicted and experimentally measured poloidal $\vec{E} \times \vec{B}$ velocities are in the range of $M_p \sim 1$. Here M_p is the poloidal Mach number, defined as $V_p B/(v_t B_p C_r)$ with B the magnetic field strength, B_p the poloidal magnetic field strength, v_t the ion thermal speed, and C_r a numerical constant of the order of unity. With such large values of V_p, it is important to take the effect of compressibility into account.

The present work is devoted to this more realistic theory of rotational bifurcation, including compressibility. The most important new physics introduced by the compressibility is the development of a shock as $M_p \sim 1$.[10,11] This paper extends the previous results from the weak shock limit $|1 - M_p| \lesssim \sqrt{\epsilon}$ to include the strong shock $|1 - M_p| \ll \sqrt{\epsilon}$, with ϵ the inverse aspect ratio. Thus, we provide a more detailed description of the evolution of the shock as M_p approaches unity.

The evolution of the shock proceeds as M_p varies, and its consequences can be tested experimentally. The shock first appears at a shock angle $\eta_0 \gtrsim \pi$ inside the torus, when $|1 - M_p| \lesssim \sqrt{\epsilon}$ if the plasma rotates counterclockwise poloidally.[10] The shock angle is the poloidal angle at which the strongest variations of plasma density and potential occur.

When M_p increases, η_0 moves in the direction of poloidal rotation. At $M_p = 1$, $\eta_0 = 2\pi$. When $M_p - 1 \lesssim \sqrt{\epsilon}$, the shock angle is at $\eta_0 \lesssim \pi$. The parallel viscosity associated with the shock reaches its maximum at $M_p = 1$; this maximum constitutes the barrier that must be overcome to have a poloidal supersonic flow. Strong up-down asymmetric components of poloidal variations of plasma density and potential develop at $M_p \simeq 1$. In the edge region, the convective poloidal momentum transport weakens the parallel viscosity and facilitates the L-H transition.

The remainder of this paper is organized as follows. In Sec. II, we derive the local (to the magnetic field $\vec{B}$) force balance equation, parallel to the magnetic field $\vec{B}$, including the parallel viscosity as the main dissipation mechanism. We assume electrons to be isothermal and ions adiabatic. The linear solution and the shock solution to the local parallel force balance equation are given in Sec. III. A prescription for obtaining the general solution to the local parallel force balance equation is given in Sec. IV. In Sec. V, we derive the evolution equations for both poloidal and toroidal rotation in tokamaks; these equations include fluxes such as ion orbit loss or anomalous viscosity that are not intrinsically ambipolar. The parallel viscosity and the convective poloidal momentum transport are evaluated with the linear and shock solutions in Sec. VI. The implications of the results for the L-H transition are discussed in Sec. VII. Concluding remarks are given in Sec. VIII.

II. LOCAL PARALLEL MOMENTUM BALANCE EQUATION

The variations of plasma density and electrostatic potential within a flux surface in axisymmetric tokamaks are governed by the local parallel (to magnetic field $\vec{B}$) momentum balance, if the effects of heat flow are neglected. In the conventional neoclassical case of slow rotation, the temperature gradient is crucial in allowing even slow poloidal motion. However, in the rapidly rotating regime considered here, the temperature gradient has no dramatic effect. Summing momentum balance equations over plasma species, and neglecting the time-dependent term, we find the parallel momentum balance equation

$$\vec{B} \cdot \vec{V} \cdot \nabla \vec{V} = -\frac{1}{NM} \vec{B} \cdot \nabla \left(P_e + P_i\right) - \frac{1}{NM} \vec{B} \cdot \nabla \cdot \overleftrightarrow{\Pi}_i \quad , \tag{1}$$

where P_e and P_i are electron and ion plasma pressure, respectively, $\overleftrightarrow{\Pi}_i$ is the ion viscous tensor, N is the plasma density, M is the ion mass, and $\vec{V}$ is plasma flow velocity. The contribution of electrons to the viscous force is neglected since it is smaller by a factor of the order of $\sqrt{M_e/M}$, with M_e the electron mass.

We assume the electron temperature to be constant along $\vec{B}$ owing to the rapid electron motion along the magnetic field line. Ions are assumed to be adiabatic because of the large poloidal flow velocity.[12] With these two assumptions, we have

$$\frac{1}{N} \vec{B} \cdot \nabla \left(P_e + P_i\right) = \left(P_e + \frac{5}{3} P_i\right) \vec{B} \cdot \vec{\nabla} \left(\ln N\right) \quad . \tag{2}$$

We use conventional tokamak flux coordinates (ψ, θ, ζ) with

$$\vec{B} = \frac{\chi'}{2\pi} \nabla\zeta \times \nabla\psi + I \nabla\zeta \quad , \tag{3}$$

where θ is the poloidal angle, ζ is the toroidal angle, ψ is the flux surface label, χ' is the poloidal flux density, $I = R^2 \vec{B} \cdot \nabla\zeta$, and R is the major radius.[13] The poloidal magnetic field $\vec{B}_p$ is $\vec{B}_p = \chi' \nabla\zeta \times \nabla\psi/(2\pi)$.

The convective term $\vec{B} \cdot \vec{V} \cdot \nabla \vec{V}$ can be rewritten as

$$\vec{B} \cdot \vec{V} \cdot \nabla \vec{V} = \frac{1}{2} \vec{B} \cdot \nabla(\vec{V} \cdot \vec{V}) + (\vec{V} \times \vec{B}) \cdot (\nabla \times \vec{V}) \quad . \tag{4}$$

If we assume $d(\ln \Phi)/d\psi \gg d(\ln N)/d\psi$, where Φ is the electrostatic potential, we have

$$\vec{V} \times \vec{B} = c \Phi' \nabla\psi \, , \tag{5}$$

where $\Phi' = d\Phi/d\psi$ and c is the speed of light. From $\nabla \cdot (N\vec{V}) = 0$, we can express the plasma flow velocity $\vec{V}$ as

$$\vec{V} = \frac{K(\psi)}{N} \vec{B} - N c \Phi' R^2 \vec{\nabla}\zeta \, , \tag{6}$$

where $K = N\vec{V} \cdot \nabla\theta / (\vec{B} \cdot \nabla\theta)$ is a flux function ψ only. Substituting Eqs. (5) and (6) into Eq. (4), we obtain

$$\vec{B} \cdot \vec{V} \cdot \nabla \vec{V} = \frac{1}{2} K^2 \vec{B} \cdot \nabla \left(\frac{B^2}{N^2} \right) - \frac{1}{2} I^2 (c\Phi')^2 \vec{B} \cdot \nabla \left(\frac{1}{B^2} \right) \quad . \tag{7}$$

Employing the Chew-Goldberger-Low form of the viscous tensor $\overleftrightarrow{\Pi} = (P_\parallel - P_\perp)(\hat{n}\hat{n} - \overleftrightarrow{I}/3)$, we obtain the parallel viscous force $\vec{B} \cdot \nabla \cdot \overleftrightarrow{\Pi}$,

$$\vec{B} \cdot \nabla \cdot \overleftrightarrow{\Pi} = \frac{2}{3} \vec{B} \cdot \nabla (P_\parallel - P_\perp) - (P_\parallel - P_\perp) \frac{\vec{B} \cdot \nabla B}{B} \quad . \tag{8}$$

The subscript for plasma species is neglected for simplicity in Eq. (8). It shall appear that the second term on the right side of Eq. (8) is smaller by $O(\epsilon)$ than the first term; we therefore neglect the second term in constructing the local parallel momentum balance equation. Other contributions to ion stress, such as gyroviscosity, are smaller by at least one power of the small gyration radius. The pressure anisotropy $(P_\parallel - P_\perp)$ in a poloidally rotating tokamak plasma, calculated from the drift kinetic equation with mass flow velocity,[14] is

$$P_\parallel - P_\perp = -2\sqrt{\pi} I_{ps} K M v_t B \left[\frac{\partial}{\partial\theta} (\ln B) - \frac{2}{3} \frac{\partial}{\partial\theta} (\ln N) \right] \quad , \tag{9}$$

where $v_t = \sqrt{2T_i/M}$ and T_i is the ion temperature.[15,16] The integral I_{ps} in Eq. (9) is

$$I_{ps} = \frac{1}{\pi} \int_0^\infty dx\, x^2 e^{-x} \int_{-1}^{1} dy \left(\frac{1}{2} - \frac{3y^2}{2} \right)^2 \frac{\nu}{U_t^2 + \nu^2} \quad , \tag{10}$$

where $\nu = \nu_T / (v_t \sqrt{x} \vec{B} \cdot \nabla\theta / B)$, $U_t = G_r \left[y + (\vec{V}_E + V_\parallel \hat{n}) \cdot \nabla\theta / (v_t \sqrt{x} \vec{B} \cdot \nabla\theta / B) \right]$, G_r is a geometric factor, $\vec{V}_E$ is the $\vec{E} \times \vec{B}$ drift velocity, $V_\parallel$ is the mass flow parallel to the magnetic field line. $x = v^2/v_t^2$, v is the speed of the particle, and $\nu_T = 3\nu_D + \nu_E$ as defined in Ref. 13. In cases with $M_p \ll 1$ and $M_p \gg 1$, $G_r = 1$; in the case of $|1 - M_p| \lesssim \sqrt{\epsilon}$, $G_r = 1/2$. The effects of the heat flow are neglected in Eq. (9).

Substituting Eqs. (2), (7), and (8) into Eq. (1), we obtain a local parallel momentum balance equation,

$$\vec{B}\cdot\nabla\left[\frac{1}{2}K^2\frac{B^2}{N^2}-\frac{1}{2}\frac{I^2(c\langle\Phi\rangle')^2}{B^2}+\frac{P_e}{NM}\ln N\right.$$
$$\left.+\frac{5}{3}\frac{\langle P_i\rangle}{\langle N^{5/3}\rangle M}N^{2/3}+\frac{2}{3}\frac{1}{\langle N\rangle M}(P_\parallel-P_\perp)\right]=0\,. \qquad (11)$$

III. LINEAR SOLUTION AND SHOCK SOLUTION

To solve Eq. (11), we integrate along the magnetic field line to obtain

$$\frac{1}{2}K^2\left(\frac{B^2}{N^2}-\left\langle\frac{B^2}{N^2}\right\rangle\right)-\frac{1}{2}I^2\left(c\langle\Phi\rangle'\right)^2\left(\frac{1}{B^2}-\left\langle\frac{1}{B^2}\right\rangle\right)+\frac{P_e}{NM}\left(\ln N-\langle\ln N\rangle\right)$$
$$+\frac{5}{3}\frac{\langle P_i\rangle}{\langle N^{5/3}\rangle M}\left(N^{2/3}-\langle N^{2/3}\rangle\right)-\frac{2}{3}\frac{1}{\langle N\rangle M}\left(P_\parallel-P_\perp\right)=0\quad , \qquad (12)$$

where the angular brackets denote the flux surface average. The integration constant has been determined by noting that the flux surface average annihilates the left side of Eq. (9). The poloidal variation of the $(1/N)$ factor in front of $\vec{B}\cdot\nabla(P_\parallel-P_\perp)$ is neglected, since it yields only an $O(\epsilon)$ correction. It is convenient to define an independent variable

$$\chi=\ln\left(N/\overline{N}\right)\quad , \qquad (13)$$

which from the Boltzmann relation is simply

$$\chi=\frac{e\tilde{\Phi}}{T_e}\quad , \qquad (14)$$

where $\tilde{\Phi}$ is the poloidally varying part of the electrostatic potential and $\bar{N}=\langle N\rangle(1-\langle\chi^2\rangle/2)$ is a convenient normalizing constant. Employing a model magnetic field $(B/B_0)=1-\epsilon\cos\theta$, assuming $\chi\sim O(\sqrt{\epsilon})$, and keeping only terms up to $O(\epsilon)$ in Eq. (12), we obtain a differential equation for χ:

$$\frac{2}{3}D\frac{d\chi}{d\theta}+(1-M_p^2)\chi+2A'(\chi^2-\langle\chi^2\rangle)=\epsilon\left[(M_p^2+2C)\cos\theta+D\sin\theta\right]\quad , \qquad (15)$$

where $D=(8\sqrt{\pi}/3)I_{ps}KB_0/(2\bar{N}v_tC_r^2)$, $M_p=KB_0/(\bar{N}v_tC_r)$, $C=I^2(c\Phi')^2/(2v_t^2B_0^2C_r^2)$, $A'=M_p^2/2+(5/18)/C_r^2$, and $C_r^2=[(5/3)+T_e/T_i]/2$.

In the linear regime, where either $M_p \ll 1$ or $M_p \gg 1$, we can neglect the nonlinear term $(\chi^2 - \langle\chi^2\rangle)$ in Eq. (15) and solve the linearized equation

$$\frac{2}{3}D\frac{d\chi}{d\theta} + (1 - M_p^2)\chi = \epsilon\left[(M_p^2 + 2C)\cos\theta + D\sin\theta\right] \quad . \tag{16}$$

Expanding $\chi = \chi_s \sin\theta + \chi_c \cos\theta$, we obtain the linear solution to Eq. (16),

$$\chi_s = \epsilon D\left[\frac{3}{2}(1 - M_p^2) + M_p^2 + 2C\right]\left[\frac{2D^2}{3} + \frac{3}{2}(1 - M_p^2)^2\right]^{-1} \quad , \tag{17}$$

$$\chi_c = \epsilon\left[\frac{3}{2}(1 - M_p^2)(M_p^2 + 2C) - D^2\right]\left[\frac{2D^2}{3} + \frac{3}{2}(1 - M_p^2)^2\right]^{-1} \quad . \tag{18}$$

These results are consistent with the linearization because when either $M_p \ll 1$ or $M_p \gg 1$, $3(1 - M_p^2)^2/2 \gg 2D^2/3$ and χ is of the order of ϵ (note that $D = 4\sqrt{\pi}I_{ps}M_p/3$.)

We note that when $M_p \gg 1$, then $M_p^2 \simeq 2C$ and Eqs. (17) and (18) imply $\chi_s \simeq 0$ and $\chi_c \simeq -2\epsilon$. This result can be understood from Eq. (11). Because $M_p \gg 1$, Eq. (11) can be written, to the lowest order in $(1/M_p)$, as

$$\vec{B}\cdot\nabla\left[\frac{1}{2}K^2\frac{B^2}{N^2} - \frac{1}{2}\left(\frac{Ic\Phi'}{B}\right)^2\right] = 0 \, . \tag{19}$$

The solution to Eq. (19) is

$$\frac{M_p^2}{2C}\left[\frac{(B/B_0)^2}{(N/\bar{N})^2} - \left\langle\frac{(B/B_0)^2}{(N/\bar{N})^2}\right\rangle\right] = \frac{1}{(B/B_0)^2} - \left\langle\frac{1}{(B/B_0)^2}\right\rangle \quad . \tag{20}$$

Because $M_p^2/2C \simeq 1$, and, in the linear regime, $N = \bar{N}(1 + \chi)$, we obtain from Eq. (20)

$$\chi = -2\epsilon\cos\theta \quad , \tag{21}$$

as in Eq. (18), for $M_p \gg 1$.

When $M_p \simeq 1$, we find from Eqs. (17) and (18)

$$\chi_s = \frac{3}{2}\epsilon\frac{(M_p^2 + 2C)}{D} \quad , \tag{22}$$

$$\chi_c = -\frac{3}{2}\epsilon \quad . \tag{23}$$

We see from Eq. (22) that $\chi_s \gtrsim 6\epsilon$ for relevant parameters $M_p^2 \sim C \gtrsim D$, and the linear solution becomes invalid when $\epsilon \lesssim 1/6$. Therefore, one must take the nonlinear term $(\chi^2 - \langle\chi^2\rangle)$ into account for typical tokamaks.

When $|1 - M_p| \lesssim \sqrt{\epsilon}$ and $2D < M_p^2\sqrt{\epsilon}$, we can solve Eq. (15) approximately to obtain a shock solution. The procedure described here is an extension of those in Refs. 10 and 11. We first simplify the right side of Eq. (15) by defining an angle ξ so that $\tan\xi = D/(M_p^2 + 2C)$ to obtain

$$\epsilon\left[(M_p^2 + 2C)\cos\theta + D\sin\theta\right] = \epsilon\sqrt{(M_p^2 + 2C)^2 + D^2}\cos(\theta - \xi) \ . \tag{24}$$

Changing the variable from θ to $\eta = \theta - \xi$, we can write Eq. (15) as

$$\frac{2}{3}D\frac{d\chi}{d\eta} + (1 - M_p^2)\chi + 2A'(\chi^2 - \langle\chi^2\rangle) = 2\epsilon G\cos\eta\,, \tag{25}$$

where $G = [(M_p^2 + 2C)^2 + D^2]^{1/2}$.

When dissipation becomes weak, i.e., $D < A'\sqrt{\epsilon}$, we can neglect the $d\chi/d\eta$ term in Eq. (25) outside the shock region, and obtain

$$\chi = \frac{-(1 - M_p^2) \pm \sqrt{(1 - M_p^2)^2 + 16A'^2[\langle X^2\rangle + (\epsilon G\cos\eta/A')]}}{4A'} \ . \tag{26}$$

Because χ is real, we must have

$$(1 - M_p^2)^2 + 16A'^2\left(\langle\chi^2\rangle + \frac{\epsilon G}{A'}\cos\eta\right) \geq 0 \tag{27}$$

for all η. This requires

$$\langle\chi^2\rangle \geq \frac{16A'\epsilon G - (1 - M_p^2)^2}{16A'^2} \ . \tag{28}$$

But we cannot have $\langle\chi^2\rangle > [16A'\epsilon G - (1 - M_p^2)^2]/(16A'^2)$, because then Eq. (26) would allow $\langle\chi\rangle = 0$ only in the presence of an even number of shocks, which is prohibited by the thermodynamic law.[10] Thus,

$$\langle\chi^2\rangle = \frac{16A'\epsilon G - (1 - M_p^2)^2}{16A'^2} \ . \tag{29}$$

Substituting Eq. (29) into Eq. (26), we obtain

$$\chi = -\frac{(1-M_p^2)}{4A'} \pm \sqrt{\epsilon \frac{G}{A'}(1+\cos\eta)} \quad . \tag{30}$$

In order to have $\langle\chi\rangle = 0$, the shock solution for the subsonic flow, $M_p < 1$, is

$$\chi = \begin{cases} -\frac{(1-M_p^2)}{4A'} + \sqrt{\epsilon \frac{G}{A'}(1+\cos\eta)}, & 0 < \eta < \pi \\ -\frac{(1-M_p^2)}{4A'} - \sqrt{\epsilon \frac{G}{A'}(1+\cos\eta)}, & \pi < \eta < \eta_0 \\ -\frac{(1-M_p^2)}{4A'} + \sqrt{\epsilon \frac{G}{A'}(1+\cos\eta)}, & \eta_0 < \eta < 2\pi \end{cases} \tag{31}$$

where η_0 is the shock angle determined from the condition $\langle\chi\rangle = 0$:

$$\sin\left(\frac{\eta_0}{2}\right) = \frac{\pi}{8}\frac{1-M_p^2}{\sqrt{2\epsilon G A'}} \quad , \tag{32}$$

with $(\pi/2) < (\eta_0/2) < \pi$. The shock solution for the supersonic flow $M_p > 1$ is

$$\chi = \begin{cases} -\frac{1-M_p^2}{4A'} - \sqrt{\epsilon \frac{G}{A'}(1+\cos\eta)}, & 0 < \eta < \eta_0 \\ -\frac{1-M_p^2}{4A'} + \sqrt{\epsilon \frac{G}{A'}(1+\cos\eta)}, & \eta_0 < \eta < \pi \\ -\frac{1-M_p^2}{4A'} - \sqrt{\epsilon \frac{G}{A'}(1+\cos\eta)}, & \pi < \eta < 2\pi \end{cases} \tag{33}$$

The shock angle η_0 for $M_p > 1$ is again determined from the condition $\langle\chi\rangle = 0$:

$$\sin\left(\frac{\eta_0}{2}\right) = \frac{\pi}{8}\frac{M_p^2-1}{\sqrt{2\epsilon G A'}} \quad , \tag{34}$$

where $0 < \eta_0/2 < \pi/2$. The jump of χ across the shock angle η_0 is

$$\Delta\chi = \chi|_{\eta\to\eta_0^+} - \chi|_{\eta\to\eta_0^-} = 2\gamma \, , \tag{35}$$

where $\gamma \equiv \sqrt{\epsilon \frac{G}{A'}(1+\cos\eta_0)}$. To find the structure of the discontinuity at the shock angle η_0, we solve Eq. (25) inside the shock region,

$$\frac{2}{3}D\frac{d\chi}{d\eta} + \left(1-M_p^2\right)\chi + 2A'\left(\chi^2 - \langle\chi^2\rangle\right) = 2\epsilon G\cos\eta_0 \quad , \tag{36}$$

with the boundary condition that $\chi = -(1-M_p^2)/(4A')$ at $\eta = \eta_0$. The solution to Eq. (36) is

$$\chi = -\frac{1-M_p^2}{4A'} + \gamma\frac{\exp[(6A'\gamma/D)(\eta-\eta_0)] - 1}{\exp[(6A'\gamma/D)(\eta-\eta_0) + 1} \quad . \tag{37}$$

It is straightforward to show that when $(\eta-\eta_0) \to \pm\infty$, the solution in Eq. (37) connects to the solutions in Eqs. (31) and (33). The results in Ref. 11 for $M_p \simeq 1$ are also reproduced in Eqs. (31), (33), and (37).

As the poloidal rotation speed increases from $1-M_p \lesssim \sqrt{\epsilon}$ to $M_p \simeq 1$, and from $M_p \simeq 1$ to $M_p - 1 \lesssim \sqrt{\epsilon}$, the shock angle η_0 and the variations of plasma density and potential also vary. When $1 - M_p \simeq \sqrt{\epsilon}$, η_0 is close to (but larger than) π and the variations of plasma density and potential are almost up-down symmetric. At $M_p \simeq 1$, η_0 is at $\theta = 0$ or 2π and the variations of plasma density and potential are up-down asymmetric. As M_p approaches $1 + \sqrt{\epsilon}$, the shock angle η_0 is close to (but smaller than) π and the variations of plasma density and potential are again almost up-down symmetric. A schematic diagram for the solution $[\chi + (1 - M_p^2)/4A']$ vs angle η as the poloidal rotation speed changes is shown in Fig. 1. The symmetry property of the poloidal variations of plasma density and potential can be measured experimentally when the poloidal flow velocity V_p is in the range of the sound velocity $v_t B_p/B$.

IV. HOPF-COLE TRANSFORMATION AND GENERAL SOLUTION

Here we return to Eq. (25) to consider its exact solution. Thus, we apply the well-known Hopf-Cole transformation[17]

$$\chi = \frac{D}{3A'}\frac{Z'}{Z} \tag{38}$$

and find that Eq. (25) is reduced to a homogeneous equation,

$$Z'' + \frac{1 - M_p^2}{2A'F} Z' - \left[\left\langle \left(\frac{Z'}{Z} \right)^2 \right\rangle + \frac{b}{F^2}\cos\eta \right] Z = 0 \quad , \tag{39}$$

where $F = D/3A'$ and $b = \epsilon G/2A'$. Indeed, Eq. (39) is a *linear* ordinary differential equation, despite the apparently nonlinear term $\langle (Z'/Z)^2 \rangle$. The point is that, from partial integration, $\langle (Z'/Z)^2 \rangle = \langle Z''/Z \rangle$, as is required by consistency of Eq. (39). Therefore, one can replace the nonlinearity by an unspecified constant without affecting the content of the equation.

As discussed in Ref. 17, at $M_p = 1$, Eq. (39) becomes a Mathieu equation,[18]

$$Z'' - \left[\left\langle \left(\frac{Z'}{Z} \right)^2 \right\rangle + \frac{b}{F^2} \cos \eta \right] Z = 0 \quad . \tag{40}$$

It is the periodic Mathieu function of order zero, ce_0,[18] that satisfies the conditions that χ must be finite and periodic. We thus obtain the exact solution at $M_p = 1$,

$$\chi = \frac{D}{3A'} \left(\frac{dce_0}{d\eta} \right) \frac{1}{ce_0} . \tag{41}$$

It is obvious that $\langle \chi \rangle = 0$. For typical parameters $A \sim C \simeq D$, $2b/F^2 \simeq 36\epsilon \gg 1$ for $\epsilon \simeq 1/4$, the solution in Eq. (41) approaches a shock-like solution. Therefore, we conclude that the shock solution is a good approximation when $M_p \simeq 1$.

Because χ and thus Z are periodic functions, the general solution for Eq. (39) can be obtained by Fourier series expansion,[17]

$$Z = a_0 + \sum_{m=1}^{\infty} (a_m \cos m\eta + b_m \sin m\eta) \quad . \tag{42}$$

Substituting Eq. (42) into Eq. (39), we obtain a set of linear equations:

$$\left\langle \left(\frac{Z'}{Z} \right)^2 \right\rangle a_0 + \frac{b}{F^2} \frac{a_1}{2} = 0 \quad ,$$

$$-\left[1 + \left\langle \left(\frac{Z'}{Z} \right)^2 \right\rangle \right] a_1 + \frac{1 - M_p^2}{2A'F} b_1 - \frac{b}{F^2} \frac{a_2}{2} = 0 \quad ,$$

$$-\left[1 + \left\langle \left(\frac{Z'}{Z} \right)^2 \right\rangle \right] b_1 - \frac{1 - M_p^2}{2A'F} a_1 - \frac{b}{F^2} \frac{b_2}{2} = 0 \quad ,$$

and for $m \geq 2$,

$$\frac{1 - M_p^2}{2A'F} m b_m + \left[-m^2 - \left\langle \left(\frac{Z'}{Z} \right)^2 \right\rangle \right] a_m - \frac{b}{F^2} \left(\frac{a_{m-1}}{2} + \frac{a_{m+1}}{2} \right) = 0 \quad ,$$

$$-\frac{1 - M_p^2}{2A'F} m a_m + \left[-m^2 - \left\langle \left(\frac{Z'}{Z} \right)^2 \right\rangle \right] b_m - \frac{b}{F^2} \left(\frac{b_{m-1}}{2} + \frac{b_{m+1}}{2} \right) = 0 \quad . \tag{43}$$

The eigenvalue $\langle (Z'/Z)^2 \rangle$ is determined by the solution of the determinant of the coefficients of Eq. (43). A similar set of equations has been solved numerically in Ref. 17 for a differential equation

$$N_{0k} Z'' + Z' - \frac{1}{2N_{0k}} \left(A_{0k} \cos \eta + \beta_{0k} \right) Z = 0 \quad , \tag{44}$$

where N_{0k}, A_{0k}, and β_{0k} are numerical constants. As the relative magnitudes of N_{0k} and A_{0k} change, the solution of Eq. (44) can have either a sinusoidal-like solution or a shock-like solution, similar to the situations discussed in Sec. III.

We employ the results of Ref. 17 to discuss the relevance of the shock solution for $1 - M_p \lesssim \sqrt{\epsilon}$. For $M_p \cong 0.65$, $(1 - M_p^2)/A' = 1$ and we can write Eq. (39) as

$$FZ'' + Z' - \frac{1}{2F} \left[2b \cos \eta + 2F^2 \left\langle \left(\frac{Z'}{Z} \right)^2 \right\rangle \right] = 0 \quad . \tag{45}$$

Comparing Eq. (45) with Eq. (44), we find $F = N_{0k}$, $2b = A_{0k}$, and $\beta_{0k} = 2F^2 \left\langle \left(\frac{Z'}{Z} \right)^2 \right\rangle$. For this case, $A_{0k} = 2b \gtrsim 4\epsilon \simeq 1$ for $\epsilon \simeq 1/4$, and $N_{0k} = F = D(3A') \lesssim 0.33$ for $A \gtrsim D$. With these values of A_{0k} and N_{0k}, we find from Fig. 6 of Ref. 17 that the exact solution has the characteristics of the shock solution when $1 - M_p \simeq 0.35 \lesssim \sqrt{\epsilon} \simeq 0.5$ for $\epsilon \simeq 1/4$. Note also that the shock angle in Fig. 6 of Ref. 17 is located in the range $\pi < \eta_0 < 2\pi$, as discussed in Sec. III and Ref. 10 for $1 - M_p \lesssim \sqrt{\epsilon}$.

V. EVOLUTION EQUATION FOR POLOIDAL AND TOROIDAL ROTATION

The evolution equation for poloidal rotation in tokamaks has been derived by several authors.[18,19] The version derived here includes the nonintrinsically ambipolar flux so that it can be employed to model the radial electric field in the edge region. Because of the steep potential gradients frequently observed in this region, a rather delicate ordering is required.

Let us denote the poloidal and toroidal flow speeds by

$$V_p \equiv (\vec{B}_p/B_p)\cdot\vec{V} \quad , V_T \equiv R\nabla\zeta\cdot\vec{V} \, .$$

We assume that

$$V_p \sim V_T \sim (B_p/B)v_T \tag{46}$$

with $B_p/B \ll 1$. This conclusion is consistent with $\vec{E}\times\vec{B}$ motion in a steep electrostatic field,

$$\nabla\Phi \sim \Phi/\rho_{pi} \, . \tag{47}$$

It is also consistent with neoclassical predictions provided we assume that toroidal or parallel damping prevents rapid toroidal flow; see, for example, Eq. (5). Note that Eqs. (46) and (47) are consistent only if

$$\nabla V \sim V/\rho_{pi} \, . \tag{48}$$

On the other hand, other plasma quantities, including the pressures and temperatures of all species, are assumed to vary slowly on the poloidal gyroradius scale:

$$\nabla P \sim P/r \ll P/\rho_{pi} \, , \text{etc.} \tag{49}$$

We will refer to the ordering described by Eqs. (46)–(49), which departs from conventional small gyroradius theory, as the *sheath ordering*. Notice in particular that Eq. (6) for the plasma flow appears, in the sheath ordering, as a consequence of small B_p/B; in conventional theory it is obtained from small ρ_{pi}/r.

Following the procedure in Ref. 19, we take the dot product of Eq. (6) with $R^2\nabla\zeta$ to obtain

$$\left\langle R^2\nabla\zeta\cdot N\vec{V}\right\rangle = KI - c\Phi'\langle R^2 N\rangle \quad . \tag{50}$$

Note that K is a function of ψ only. Substituting Eq. (50) into Eq. (6), we find

$$N\vec{V} = K\vec{B} + \frac{N}{\langle R^2 N\rangle}\left[\langle R^2\nabla\zeta\cdot N\vec{V}\rangle - KI\right] R^2\nabla\zeta \ . \tag{51}$$

We combine Eq. (50) with the general plasma acceleration law

$$MN\frac{\partial}{\partial t}\vec{V} + MN\vec{V}\cdot\nabla\vec{V} + \nabla(P_e + P_i) + \nabla\cdot\overleftrightarrow{\Pi} + \vec{\Xi} = \frac{1}{c}\vec{J}\times\vec{B} - \nu_{\text{eff}} MN\vec{V} \ , \tag{52}$$

in which an effective damping frequency ν_{eff} is used to model momentum loss associated with charge exchange and anomalous momentum losses, and the force $\vec{\Xi}$ to model the momentum source or sink associated with ion orbit loss. The result is

$$\begin{aligned}
&\frac{\langle N\rangle}{\langle B_p^2\rangle}\left(\left\langle\frac{B^2}{N}\right\rangle - \frac{I^2}{\langle R^2 N\rangle}\right)\frac{\partial}{\partial t}\left(\frac{\langle N\vec{V}\cdot\vec{B}_p\rangle}{\langle N\rangle}\right) \\
&= -\frac{I}{\langle R^2 N\rangle}\frac{\partial}{\partial t}\langle R^2\nabla\zeta\cdot N\vec{V}\rangle - \langle\vec{B}\cdot\vec{V}\cdot\nabla\vec{V}\rangle - \frac{1}{M}\left\langle\frac{\vec{B}\cdot\nabla\cdot\overleftrightarrow{\Pi}}{N}\right\rangle - \frac{1}{M}\left\langle\frac{\vec{B}\cdot\vec{\Xi}}{N}\right\rangle \\
&\quad - \nu_{\text{eff}}\langle\vec{B}\cdot\vec{V}\rangle \, .
\end{aligned} \tag{53}$$

The contribution of electrons to Eq. (53) is neglected. The relaxation of the toroidal angular momentum is governed by

$$\begin{aligned}
\frac{\partial}{\partial t}\left(\left\langle R^2\nabla\zeta\cdot N\vec{V}\right\rangle\right) &= \frac{1}{cM}\left\langle R^2\nabla\zeta\cdot\vec{J}\times\vec{B}\right\rangle - \nu_{\text{eff}}\left\langle R^2\nabla\zeta\cdot N\vec{V}\right\rangle \\
&\quad - \left\langle R^2\nabla\zeta\cdot\nabla\cdot\overleftrightarrow{\Pi}\right\rangle - \left\langle R^2\nabla\zeta\cdot N\vec{V}\cdot\nabla\vec{V}\right\rangle \\
&\quad - \frac{1}{M}\left\langle\frac{I}{B^2}\vec{B}\cdot\vec{\Xi}\right\rangle - \frac{1}{cM}\left\langle\vec{J}_{\text{orb}}\cdot\nabla\psi\right\rangle \ .
\end{aligned} \tag{54}$$

Here, $\vec{J}_{\text{orb}}$ is the radial current associated with the nonintrinsically ambipolar particle flux $\vec{\Gamma}_{\Xi}$ driven by the force $\vec{\Xi}$ and is defined as $\langle\vec{J}_{\text{orb}}\cdot\nabla\psi\rangle = e\langle\vec{\Gamma}_{\Xi}\cdot\nabla\psi\rangle = c\langle\nabla\psi\cdot\vec{B}\times\vec{\Xi}/B^2\rangle$. We employ $\langle R^2\nabla\zeta\cdot\nabla\cdot\overleftrightarrow{\Pi}\rangle$ in Eq. (54) to denote the classical and neoclassical viscosities, which are small and will be neglected.[12] The plasma current density $\langle R^2\nabla\zeta \cdot \vec{J}\times\vec{B}\rangle$ can be expressed in terms of $\partial(\vec{E}\cdot\nabla\psi)/\partial t$ from the charge continuity equation to obtain[19]

$$\left\langle R^2\nabla\zeta\cdot\vec{J}\times\vec{B}\right\rangle = \left\langle\vec{J}\cdot\nabla\psi\right\rangle = -\frac{1}{4\pi}\left\langle\frac{\partial\vec{E}}{\partial t}\cdot\nabla\psi\right\rangle \quad . \tag{55}$$

Substituting Eqs. (54) and (55) into Eq. (53), we obtain the evolution equation for the poloidal rotation,[20]

$$\begin{aligned}
\frac{\langle N\rangle}{\langle B_p^2\rangle}&\left(\left\langle\frac{B^2}{N}\right\rangle - \frac{I^2}{\langle R^2N\rangle}\right)\frac{\partial}{\partial t}\left(\frac{\langle N\vec{V}\cdot\vec{B}_p\rangle}{\langle N\rangle}\right) - \frac{I}{\langle R^2N\rangle cM4\pi}\left\langle\frac{\partial\vec{E}}{\partial t}\cdot\nabla\psi\right\rangle\\
&= \frac{I}{\langle R^2N\rangle cM}\left\langle\vec{J}_{\mathrm{orb}}\cdot\nabla\psi\right\rangle + \frac{I}{\langle R^2N\rangle}\left\langle R^2\nabla\zeta\cdot N\vec{V}\cdot\nabla\vec{V}\right\rangle\\
&\quad - \left\langle\vec{B}\cdot\vec{V}\cdot\nabla\vec{V}\right\rangle - \frac{1}{M}\left\langle\frac{\vec{B}\cdot\nabla\cdot\overleftrightarrow{\Pi}}{N}\right\rangle\\
&\quad + \left\langle\left(\frac{I^2}{\langle R^2N\rangle MB^2} - \frac{1}{NM}\right)\vec{B}\cdot\Xi\right\rangle\\
&\quad - \nu_{\mathrm{eff}}\left\langle\vec{B}_p\cdot\vec{V}\right\rangle \quad .
\end{aligned} \tag{56}$$

The $\langle\partial\vec{E}/\partial t\cdot\nabla\psi\rangle$ term is a factor of V_A^2/c^2 smaller than the $\partial(\langle N\vec{V}\cdot\vec{B}_p\rangle/\langle N\rangle)/\partial t$ term and can be neglected in general. We note that because $\nabla\psi = -(2\pi R^2/I\chi')\vec{B}\times\vec{B}_p$, $\langle\vec{J}_{\mathrm{orb}}\cdot\nabla\psi\rangle$ can also be interpreted as the poloidal component of the torque $e\vec{\Gamma}\times\vec{B}$.

The inertia enhancement factor $M_{\mathrm{eff}} = \left(\langle N\rangle/\langle B_p^2\rangle\right)\left(B^2/N\rangle - I^2/\langle R^2N\rangle\right)$ in Eq. (53) can be calculated to obtain

$$M_{\mathrm{eff}} = 1 + q^2\left(2 + \frac{2}{\epsilon}\langle\chi\cos\theta\rangle + \frac{1}{\epsilon^2}\langle\chi^2\rangle\right) . \tag{57}$$

In the linear regime, we obtain

$$M_{\mathrm{eff}} = 1 + q^2\left[2 + \frac{1}{\epsilon}\chi_c + \frac{1}{2\epsilon^2}\left(\chi_c^2 + \chi_s^2\right)\right] \quad . \tag{58}$$

In the $M_p \ll 1$ limit, we reproduce the well-known result $M_{\mathrm{eff}} \simeq 1 + 2q^2$. In the $M_p \gg 1$ limit, we employ Eq. (21) to obtain $M_{\mathrm{eff}} = 1 + q^2$. In the case of $|M_p - 1| \ll \sqrt{\epsilon}$, we find, from the strong shock solution,

$$M_{\mathrm{eff}} \cong 1 + \frac{2q^2}{\epsilon} \tag{59}$$

for $A' \sim C$. In the range of M_p of interest, the inertia enhancement factor is generally large, $M_{\text{eff}} \gtrsim q^2 \gg 1$.

It is appropriate to comment here on the rotation damping term in (52). It serves to account for turbulent viscosity, as well as atomic physics effects, such as charge exchange. The small parallel plasma velocity commonly observed in tokamak experiments indicates that damping may dominate the flux-surface averaged, parallel momentum equation,

$$\left\langle M\left(\frac{\partial}{\partial t}\right) N V_{\parallel}\right\rangle + M\langle NB\cdot(\vec{V}\cdot\nabla\vec{V})\rangle + \langle\vec{B}\cdot\nabla\cdot\overleftrightarrow{\Pi}\rangle = -\nu_{\text{eff}} M \left\langle NBV_{\parallel}\right\rangle \tag{60}$$

thus forcing

$$\left\langle NBV_{\parallel}\right\rangle = 0\,. \tag{61}$$

Notice that the other terms in Eq. (60) are quite small—the parallel pressure gradient terms, in particular, have been annihilated by the average—so that Eq. (61) does not require ν_{eff} to be large. Indeed, Eq. (61) pertains for the experimentally consistent case,

$$\nu_{\text{eff}} \sim \nu_{c}\,, \tag{62}$$

where ν_c is the Coulomb collision frequency. For this reason, and because of the shock ordering $\tilde{N}/N \gg r/R$, rotation damping does not dominate the lowest order, unaveraged equation, (11). Therefore, the lowest order shock structure of Eq. (15) *et seq.* is unchanged.

On the other hand, rotation damping indirectly alters the description of the shock. The point is that Eq. (61) forces the parameter K, describing the poloidal velocity, to have the value

$$K = c\left(\frac{d\Phi}{d\psi}\right)\langle N\rangle I/\langle B^2\rangle \approx c\left(\frac{d\Phi}{d\psi}\right)\tilde{N}\,R_0/B_0\,. \tag{63}$$

The result is to simplify many of the formulae in Sec. III, primarily by allowing the substitution

$$2C \to M_p^2 \,. \tag{64}$$

Thus the shock description of Sec. III, which pertains for a general flow of the form (51), is straightforwardly specialized to the strongly damped case.

VI. PARALLEL VISCOSITY AND CONVECTIVE MOMENTUM TRANSPORT

If there are no nonintrinsically ambipolar fluxes, such as $J_{\rm orb}$, and no anomalous momentum loss mechanisms, the evolution of poloidal rotation is governed by the parallel viscosity $\langle \vec{B}\cdot\nabla\cdot\overleftrightarrow{\Pi}/N\rangle$ and convective momentum transport $\langle \vec{B}\cdot\vec{V}\cdot\nabla\vec{V}\rangle$. With the linear solution and shock solution given in Sec. III, we can evaluate $\langle \vec{B}\cdot\nabla\cdot\overleftrightarrow{\Pi}/N\rangle$, $\langle \vec{B}\cdot\vec{V}\cdot\nabla\vec{V}\rangle$, and $\langle R^2\nabla\zeta\cdot N\vec{V}\cdot\nabla\vec{V}\rangle$.

From Eq. (8), we find

$$\left\langle \frac{\vec{B}\cdot\nabla\cdot\overleftrightarrow{\Pi}}{N}\right\rangle = \left(\frac{2}{3}\right)\left\langle \frac{\vec{B}\cdot\nabla(P_{\parallel}-P_{\perp})}{N}\right\rangle - \left\langle \frac{(P_{\parallel}-P_{\perp})}{N}\frac{\vec{B}\cdot\nabla B}{B}\right\rangle \,. \tag{65}$$

Integrating by parts, we obtain, from Eq. (55), the parallel viscosity,

$$\left\langle \frac{\vec{B}\cdot\nabla\cdot\overleftrightarrow{\Pi}}{N}\right\rangle = -\left\langle \frac{(P_{\parallel}-P_{\perp})}{N}\left[\vec{B}\cdot\nabla(\ln B) - \frac{2}{3}\vec{B}\cdot\nabla(\ln N)\right]\right\rangle \,. \tag{66}$$

Substituting Eq. (9) into Eq. (66), we obtain a positive definite form for the parallel viscosity,

$$\left\langle \frac{\vec{B}\cdot\nabla\cdot\overleftrightarrow{\Pi}}{N}\right\rangle = 2\sqrt{\pi}I_{ps}K\,Mv_tB\left\langle\left(\frac{\vec{B}\cdot\nabla\theta}{N}\right)\left[\frac{\partial}{\partial\theta}(\ln B) - \frac{2}{3}\frac{\partial}{\partial\theta}(\ln N)\right]^2\right\rangle \,. \tag{67}$$

To the lowest order in the large-aspect-ratio expansion, we can neglect the density and magnetic field variations in the factor $(\vec{B}\cdot\nabla\theta/N)$ inside the angular brackets in Eq. (67). Substituting the linear solution in Eqs. (17) and (18) into Eq. (67) and employing $\partial(\ln B)/\partial\theta = \epsilon\sin\theta$, we obtain

$$\left\langle \frac{\vec{B}\cdot\nabla\cdot\overleftrightarrow{\Pi}}{N} \right\rangle_{M_p \gg 1, M_p \ll 1} = \sqrt{\pi} I_{ps} K M v_t B \frac{\vec{B}\cdot\nabla\theta}{N} \left[\left(\epsilon + \frac{2}{3}\chi_c \right)^2 + \left(\frac{2}{3}\chi_s \right)^2 \right] \quad . \tag{68}$$

When $|1 - M_p| \lesssim \sqrt{\epsilon}$, we can calculate the parallel viscosity approximately with the shock solution in Eqs. (31) and (33) to obtain

$$\left\langle \frac{\vec{B}\cdot\nabla\cdot\overleftrightarrow{\Pi}}{N} \right\rangle = \left\langle \frac{\vec{B}\cdot\nabla\cdot\overleftrightarrow{\Pi}}{N} \right\rangle_{\text{shock}} + \frac{\sqrt{\pi}}{9} K\, M v_t I_{ps} \left\langle B \frac{\vec{B}\cdot\nabla\theta}{N} \right\rangle \epsilon \left(\frac{M_p^2 + 2C}{A'} \right) \quad , \tag{69}$$

where the contributions from the shock region to parallel viscosity are

$$\left\langle \frac{\vec{B}\cdot\nabla\cdot\overleftrightarrow{\Pi}}{N} \right\rangle_{\text{shock}} = \frac{2}{3\pi} M v_t^2 \left(\frac{5}{3} + \frac{T_e}{T_i} \right) \left\langle \vec{B}\cdot\nabla\theta \right\rangle A' \gamma^3 \frac{K}{|K|} \quad . \tag{70}$$

We have neglected the contribution of $\partial B/\partial\theta$ to parallel viscosity in Eq. (69) because it is formally a factor of ϵ smaller than that of $\partial N/\partial\theta$. We have also approximated $G \simeq M_p^2 + 2C$. We note that the shock viscosity in Eq. (70) is independent of collisionality, in contrast to the conventional neoclassical viscosity. For $M_p - 1 = O(\epsilon^{1/2})$, Eqs. (32), (34), and (35) show that the right side of Eq. (70) is proportional to

$$\left\{ 1 + 2C - \left(\frac{\pi}{8} \right)^2 \frac{(M_p^2 - 1)^2}{\epsilon\left[1 + (5/9C_r^2)\right]} \right\}^{3/2} \quad .$$

Hence, the shock viscosity reaches its maximum at $M_p = 1$, which is the irreducible minimum that must be overcome to have a supersonic poloidal flow. The contribution from the region outside the shock, the second term on the right side of Eq. (69), depends on the collisionality just like the conventional neoclassical viscosity. It vanishes as the ion collision frequency approaches zero.

The convective momentum transport associated with the term $\langle \vec{B}\cdot\vec{V}\cdot\nabla\vec{V}\rangle$ and $\langle R^2\nabla\zeta\cdot N\vec{V}\cdot\nabla\vec{V}\rangle$ are driven by the coupling between the variations of mass flows with those of plasma density and magnetic curvature.[10,22] From the elementary vector identity, we have

$$\langle \vec{B}\cdot\vec{V}\cdot\nabla\vec{V}\rangle = \langle \vec{V}\times\vec{B}\cdot\nabla\times\vec{V}\rangle \quad . \tag{71}$$

Employing the adiabatic law for ions, realizing $\vec{V} \times \vec{B} = c\vec{\nabla} P_i/(Ne) + c\vec{\nabla}\Phi + cM\vec{V}\cdot\vec{\nabla}\vec{V}/e + c\vec{\nabla}\cdot \overleftrightarrow{\pi}/(Ne)$, we find

$$\left\langle \vec{B}\cdot\vec{V}\cdot\nabla\vec{V}\right\rangle = +3\frac{c}{e}\left[\frac{I}{N}\frac{\partial K}{\partial\psi} + \frac{1}{2}\frac{\partial}{\partial\psi}\left\langle R^2\vec{\nabla}\zeta\cdot\vec{V}\right\rangle\right]\left\langle\frac{\vec{B}\cdot\vec{\nabla}\cdot\overleftrightarrow{\Pi}}{N}\right\rangle$$

and

$$\left\langle R^2\nabla\zeta\cdot N\vec{V}\cdot\nabla\vec{V}\right\rangle = \frac{3}{2}\frac{c}{e}\frac{I^2}{B^2}\frac{\partial K}{\partial\psi}\left\langle\frac{\vec{B}\cdot\nabla\cdot\overleftrightarrow{\Pi}}{N}\right\rangle, \tag{72}$$

for $|1 - M_p| \lesssim \sqrt{\epsilon}$. When $|1 - M_p| \lesssim \sqrt{\epsilon}$, the convective poloidal momentum transport is a factor of ρ_{pi}/L_p smaller than parallel viscosity in the bulk region of the plasma. Here, L_p is the radial scale length of V_p. However, in the edge region $\rho_{pi}/L_p \sim 1$, the convective poloidal momentum transport becomes as important as the parallel viscosity. In the edge region, the convective poloidal momentum transport weakens the parallel viscosity and facilitates the L-H transition.

VII. IMPLICATIONS FOR L-H TRANSITION

The measured poloidal Mach numbers M_p in the edge regions of CCT, JFT2-M, TEXTOR, and DIII-D are either close to or higher than unity.[7,8,23,24] According to the theory developed here and in Refs. 10 and 11, shocks should exist in these devices. Shocks are characterized by strong variations in poloidal plasma density and potential at the shock angle η_0 and by the development of up-down asymmetric poloidal density and potential variations at $M_p \sim 1$. When $1 - M_p \lesssim \sqrt{\epsilon}$, the shock angle η_0 is located at $\eta_0 \gtrsim \pi$. As M_p approaches unity, the shock angle moves in the direction of the poloidal rotation, as shown in Fig. 1. At $M_p = 1$, η_0 is at 2π. When $M_p - 1 \lesssim \sqrt{\epsilon}$, the shock angle is at $\eta_0 \lesssim \pi$. Furthermore, the closer M_p is to unity, the stronger the up-down asymmetric components of the poloidal variations of density and potential are. Both the movement of η_0 and the magnitude of the up-down asymmetric components of the poloidal variations of density and potential as M_p varies can be measured experimentally. Figure 2 is a schematic diagram that describes the evolution of the poloidal variation of the plasma density for different values of M_p (from $M_p \ll 1$ to $M_p \gg 1$) based on the theory developed in this paper.

The relevance of the concept of a viscosity barrier to the L-H transition has been established both experimentally and theoretically. With the development of the shock theory, a further quantitative comparison of theory and experiment can be performed. In particular, in the bulk region, the effect of the convective poloidal momentum transport is weak and plasmas are rather collisionless, i.e., $\nu_{*i} \ll 1$. Then one expects the shock barrier, which is the shock viscosity at $M_p = 1$, to become the relevant force barrier that must be overcome for supersonic poloidal flow. With an external poloidal torque, one can test the magnitude of the shock barrier experimentally.

With the shock theory developed here, one can easily modify the theory of the L-H transition proposed in Ref. 5.

VIII. CONCLUDING REMARKS

We have solved the parallel momentum balance equation with parallel viscosity as the main dissipation mechanism. For simplicity, we have neglected the effects of heat flow. We find that for parameters relevant to experiment the solution has the characteristic feature of a shock when the poloidal Mach number M_p is close to unity. The shock angle η_0 moves in the direction of the poloidal flow from $\eta_0 \gtrsim \pi$. to 2π, and then to $\eta_0 \lesssim \pi$ as M_p increases from $1 - M_p \lesssim \sqrt{\epsilon}$, to $|1 - M_p| \ll \sqrt{\epsilon}$, and then to $M_p - 1 \lesssim \sqrt{\epsilon}$. Also, strong up-down asymmetric components of poloidal density and potential variations develop when $M_p \simeq 1$. All these features can be tested experimentally during the L-H transition.

Plasma parallel viscosity and convective poloidal momentum transport are calculated based on the shock theory. We find that there exists a collisionality-independent shock viscosity when $|1 - M_p| \lesssim \sqrt{\epsilon}$. The shock viscosity reaches its maximum at $M_p = 1$, which is the critical value that must be overcome to achieve a supersonic poloidal flow. The convective poloidal momentum transport is usually smaller than the parallel viscosity by a factor of ρ_{pi}/L_p. However, in the edge region $\rho_{pi} \sim L_p$; therefore, the convective poloidal momentum transport weakens the parallel viscosity and facilitates the L-H transition.

ACKNOWLEDGMENTS

Part of this work was performed while one of the authors (KCS) was a Visiting Professor at the National Institute for Fusion Science at Nagoya, Japan. He thanks Director General A. Iiyoshi and Director T. Sato for the invitation and his colleagues for their hospitality. The author also wishes to thank Professor M. Wakatani for useful discussions.

This work was supported by the Office of Fusion Energy, U.S. Department of Energy, under contract DE-AC05-84OR21400 with Martin Marietta Energy Systems, Inc., and under contract DE-FG05-80ET-53088 with the University of Texas at Austin.

ACKNOWLEDGMENTS

1. F. Wagner, G. Becker, K. Behringer, D. Campbell, A. Eberhagen, W. Engelhardt, G. Fussmann, O. Gehre, J. Gernhardt, G. V. Gierke, G. Hass, M. Huang, F. Karger, M. Keilhacker, O. Klüber, M. Kornherr, K. Lackner, G. Lisitano, G. G. Lister, H. M. Mayer, M. Meisel, E. R. Müller, H. Murmann, N. Niedermeyer, W. Poschenrieder, H. Rapp, H. Röhr, F. Schneider, G. Siller, E. Speth, A. Stäbler, K. H. Steuer, G. Benus, O. Vollmer, and Z. Yü, Phys. Rev. Lett. **42**, 1408 (1982).
2. T. Ohkawa, M. S. Chu, F. L. Hinton, C. S. Liu, and Y. C. Lee, Phys. Rev. Lett **51**, 2101 (1983).
3. S. Saito, T. Kobayashi, M. Sugihara, T. Hirayama, and N. Fujisawa, Nucl. Fusion **25**, 829 (1985).
4. S.-I. Itoh and K. Itoh, Phys. Rev. Lett. **60**, 2276 (1988).
5. K. C. Shaing, Phys. Fluids **31**, 2249 (1988); K. C. Shaing, W. A. Houlberg, and E. C. Crume, Comments Plasma Phys. Controlled Fusion **12**, 69 (1988).
6. A. B. Hassam, T. M. Antonsen, Jr., J. F. Drake, and C. S. Liu, submitted for publication, 1990.
7. R. J. Groebner, P. Gohil, K. H. Burrell, T. H. Osborne, R. P. Seraydarian, and H. St. John, in *Proceedings of the Sixteenth European Conference on Controlled Fusion and Plasma Physics*, Venice, 1989 (European Physical Society, Petit-Lancy, Switzerland, 1989), Vol. 13B, Part I, p. 245; R. J. Groebner, K. H. Burrell, and R. P. Seraydarian, Phys. Rev. Lett. **64**, 3015 (1990).
8. R. J. Taylor, M. L. Brown, B. D. Fried, H. Grote, J. R. Liberati, G. J. Morales, P. Pribyl, D. Darrow, and M. Ono, Phys. Rev. Lett. **63**, 2365 (1989); R. J. Taylor, R. W. Conn, B. D. Fried, R. Lehmer, J. R. Liberati, P. Pribyl, L. Schmitz, G. Tynan, B. Wells, D. Darrow, and M. Ono, in *Proceedings of the Thirteenth International Conference on Plasma Physics and Controlled Nuclear Fusion Research*, Washington, D.C., 1990 (International Atomic Energy Agency, Vienna, in press).

9. K. C. Shaing and E. C. Crume, Phys. Rev. Lett. **63**, 2369 (1989); K. C. Shaing, E. C. Crume, and W. A. Houlberg, Phys. Fluids B **2**, 1402 (1990).
10. R. D. Hazeltine, E. P. Lee, and M. N. Rosenbluth, Phys. Fluids **14**, 361 (1971); N. K. Winson, J. L. Johnson, and J. M. Dawson, J. Comput. Phys. **6**, 430 (1970); J. M. Greene, J. L. Johnson, K. E. Weimer, and N. K. Winsor, Phys. Fluids **14**, 1258 (1971).
11. J. M. Greene and N. K. Winsor, Phys. Fluids **16**, 863 (1973).
12. R. D. Hazeltine and A. A. Ware, Phys. Fluids **19**, 1163 (1976).
13. S. P. Hirshman and D. J. Sigmar, Nucl. Fusion **21**, 1079 (1981).
14. R. D. Hazeltine and A. A. Ware, Plasma Phys. **20**, 673 (1978).
15. K. C. Shaing and D. A. Spong, Phys. Fluids B **2**, 1190 (1990).
16. K. C. Shaing, Phys. Fluids B **2**, 2847 (1990).
17. M. Okamura and T. Kawahara, J. Phys. Soc. Jpn. **52**, 3800 (1983).
18. A. Abramovitz and I. A. Stegun, Handbook of Mathematical Functions (Dover, New York, 1968), p. 722.
19. S. P. Hirshman, Nucl. Fusion **18**, 917 (1976).
20. A. A. Ware and J. C. Wiley, Phys. Fluids **24**, 936 (1981).
21. K. H. Burrell, T. N. Carlstrom, E. J. Doyle, P. Gohil, R. J. Groebner, T. Lehecka, N. C. Luhmann, Jr., H. Matsumoto, T. H. Osborne, W. A. Peebles, and R. Philipona, Phys. Fluids B **2**, 1405 (1990).
22. T. E. Stringer, Phys. Rev. Lett. **22**, 770 (1969).
23. K. Ida, S. Hidekuma, Y. Miura, T. Fujita, M. Mori, K. Hoshino, N. Suzuki, T. Yamauchi, and JFT-2M Group, Phys. Rev. Lett. **65**, 1364 (1990).
24. R. R. Weynants, R. J. Taylor, P. E. Vandenplas, F. Durodié, B. Schweer, D. Bora, T. Delvigne, J. Devos, K. H. Dippel, M. Gaigneaux, B. Giesen, Y. T. Lie, A. M. Messiaen, R. Moyer, U. Samm, R. P. Xchorn, C. Stickelmann, R. Van Nieuwenhove, G. Van Oost, G. H. Wolf, J. W. Yang, in *Proceedings of the Seventeenth European*

Conference on Controlled Fusion and Plasma Physics, Amsterdam, 1990 (European Physical Society, Petit-Lancy, Switzerland, 1990), Vol. 14, Part I, p. 287.

FIGURE CAPTIONS

Fig. 1. The variation of potential $[\chi(1 - M_p^2)/4A']$ vs angle η for three different values of Mach number M_p. As M_p increases, the shock angle η_0 varies from $\pi < \eta_0 < 2\pi$ for $1 - M_p \lesssim \sqrt{\epsilon}$ (a) to $\eta_0 = 2\pi$ for $M_p = 1$ (b) and to $0 < \eta_0 < \pi$ for $M_p - 1 \lesssim \sqrt{\epsilon}$ (c).

Fig. 2. Schematic diagram of the variation of plasma density with angle η for seven different values of Mach number M_p, as M_p increases from (a) $M_p < 1 - \sqrt{\epsilon}$ to (b) $1 - M_p \simeq \sqrt{\epsilon}$ at the onset of the shock to (c) $1 - M_p < \sqrt{\epsilon}$ for shock angle η_0 in the range $\pi < \eta_0 < 2\pi$ to (d) $M_p = 1$ for $\eta_0 = 2\pi$ to (e) $M_p - 1 < \sqrt{\epsilon}$ for $0 < \eta_0 < \pi$ to (f) $M_p - 1 \simeq \sqrt{\epsilon}$ for $\eta_0 = \pi$ to (g) $M_p > 1 + \sqrt{\epsilon}$. For simplicity, we assume that there is no dissipation in the system. Note that in cases (a) and (g), the density variations are approximately simple sine and cosine functions described by Eqs. (17) and (18).

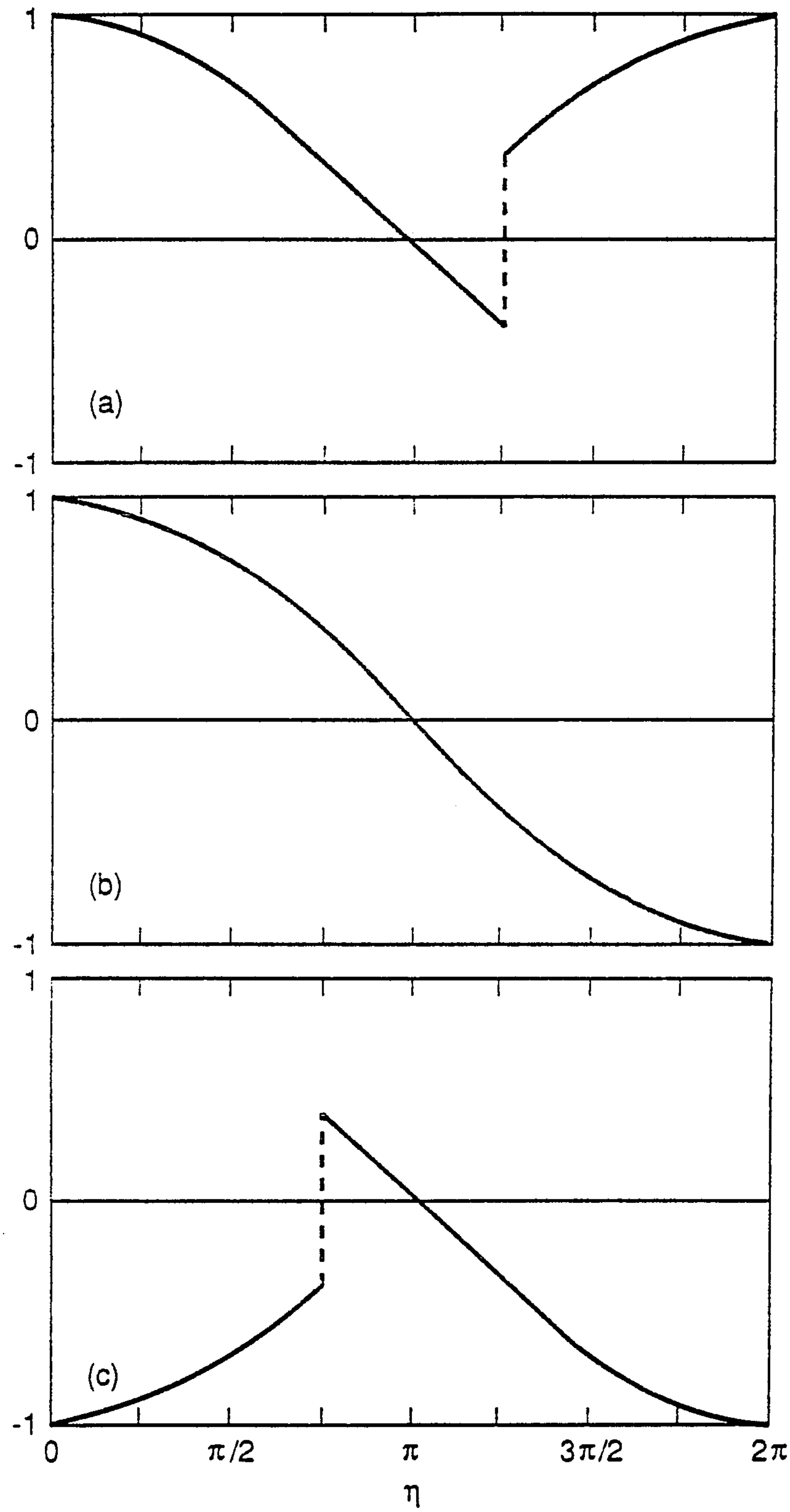

Fig. 1

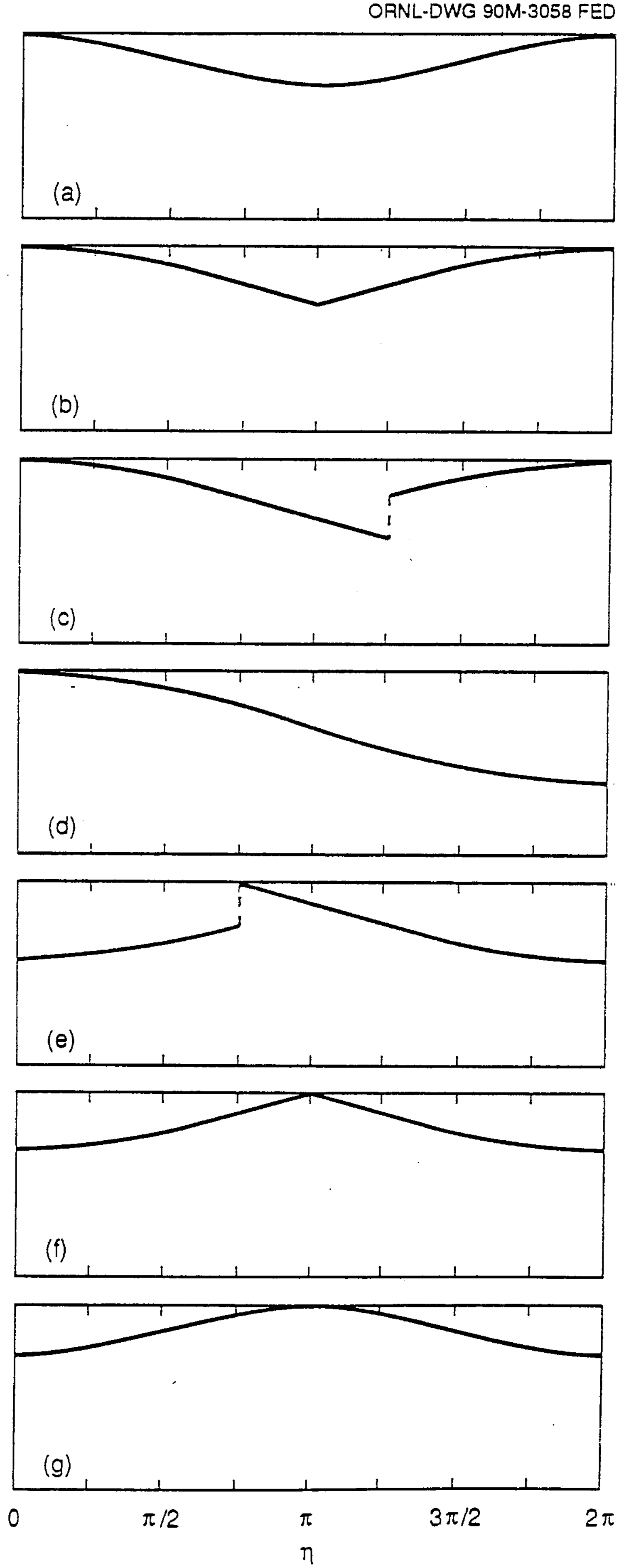

Fig. 2